Developmental Biology **238,** 274–288 (2001)
doi:10.1006/dbio.2001.0393, available online at http://www.idealibrary.com on IDEAL®

Zebrafish Early Macrophages Colonize Cephalic Mesenchyme and Developing Brain, Retina, and Epidermis through a M-CSF Receptor-Dependent Invasive Process

Philippe Herbomel,*[,1] Bernard Thisse,† and Christine Thisse†

**Unité de Génétique des Déficits Sensoriels, URA 1968 du CNRS, Département des Biotechnologies, Institut Pasteur, 25 rue du Dr Roux, 75724 Paris Cedex 15, France; and*
†Institut de Génétique et de Biologie Moléculaire et Cellulaire, CNRS/INSERM/ULP, BP 163, 67404 Illkirch Cedex, C.U. de Strasbourg, France

The origin of resident (noninflammatory) macrophages in vertebrate tissues is still poorly understood. In the zebrafish embryo, we recently described a specific lineage of early macrophages that differentiate in the yolk sac before the onset of blood circulation. We now show that these early macrophages spread in the whole cephalic mesenchyme, and from there invade epithelial tissues: epidermis, retina, and brain—especially the optic tectum. In the *panther* mutant, which lacks a functional *fms* (M-CSF receptor) gene, early macrophages differentiate and behave apparently normally in the yolk sac, but then fail to invade embryonic tissues. Our video recordings then document for the first time the behavior of macrophages in the invaded tissues, revealing the striking propensity of early macrophages in epidermis and brain to wander restlessly among epithelial cells. This unexpected behavior suggests that tissue macrophages may be constantly "patrolling" for immune and possibly also developmental and trophic surveillance. At 60 h post-fertilization, all macrophages in the brain and retina undergo a specific phenotypic transformation, into "early (amoeboid) microglia": they become more highly endocytic, they down-regulate the *L-plastin* gene, and abruptly start expressing high levels of apolipoprotein E, a well-known neurotrophic lipid carrier.

Key Words: **macrophages; macrophage motility; embryogenesis; zebrafish; microglia; epidermis; apolipoprotein E; fms; M-CSF/CSF-1.**

We recently described the emergence in the zebrafish embryo of early macrophages, well before any other leukocytes (Herbomel *et al.*, 1999). These macrophages originate from the rostralmost lateral mesoderm, just anterior to the cardiac field. They differentiate in the yolk sac. Then, some join the blood circulation, while many migrate to the head of the embryo.

Similar early macrophages were found to differentiate in the yolk sac of mammals and birds, and then to spread in the embryo's head (Takahashi *et al.*, 1989, 1996; Sorokin *et al.*, 1992a,b; Cuadros *et al.*, 1992, 1993; Lichanska and Hume, 2000). They share with zebrafish early macrophages other atypical characteristics, relative to "classical" monocyte-derived macrophages: they differentiate through a rapid pathway that appears to bypass the monocytic series, and retain a proliferative potential once they have differentiated.

Because macrophages produce an impressive range of growth factors, matrix-remodeling proteins, and all the corresponding inhibitors, under various circumstances in the adult animal, e.g., to promote tissue repair, it has recurrently been suggested that they might contribute as well to regulating the development of the organism (Gordon, 1995). Such a prospect appears even more attractive now that the existence and specificity of the early macrophage lineage has been recognized in several vertebrates. To evaluate their roles in zebrafish organogenesis, we document here their spatio-temporal deployment and behaviors in embryonic tissues. Thanks to the small size and transparency of the zebrafish embryo, we present the first live recordings of macrophage behaviors in vertebrate embry-

[1] To whom correspondence should be addressed. Fax: 33 1 45 67 69 78. E-mail: herbomel@pasteur.fr.

0012-1606/01 $35.00

onic tissues. By combining vital staining with *in situ* hybridization, we show that a major phenotypic transformation is undergone simultaneously by all early macrophages in brain and retina. Finally, we demonstrate the requirement for a functional M-CSF receptor for the invasive colonization of embryonic tissues by early macrophages.

MATERIALS AND METHODS

Observation of Live Embryos; Vital Staining with Neutral Red

DIC video microscopy was performed as previously described (Herbomel *et al.*, 1999).

Optimal staining of macrophages in live embryos was obtained by incubating embryos in 2.5 μg/ml neutral red (in embryo medium) at 25–30°C in the dark for 5–8 h. Although neutral red is well known for its ability to concentrate in lysosomes, we checked that the same refractile granules that take up neutral red in zebrafish early macrophages also show red fluorescence upon acridine orange incorporation (Allison and Young, 1969).

Apoptotic bodies were readily identified by DIC microscopy. Although vital staining with acridine orange is more widely used to score embryos for apoptotic bodies, as bright green fluorescent spots visible under the dissecting scope (Rodriguez and Driever, 1997), we always combined it with DIC microscopic identification, which we found to provide a more accurate picture of apoptotic events; only about one-fourth of apoptotic bodies visible by DIC microscopy incorporate acridine orange—most probably those containing DNA.

In Situ Hybridization and Histology

Whole-mount *in situ* hybridization, performed as described previously (Herbomel *et al.*, 1999), was carried out on embryos at the following stages: 22, 25, 30, 35, 40, 48, 60, 72, 96, 120, and 144 hpf. Several embryos at every stage were analyzed as whole mounts by high-resolution DIC video microscopy, and at least two embryos of each stage from 25 to 48 hpf were embedded in Epon or Epon-Araldite and serially sectionned in their entirety (5-μm-thick cross sections).

Double *in situ* hybridization was performed according to Hauptmann and Gerster (1994).

The *apoE*, *L-plastin*, and *fms* probes have been described (Babin *et al.*, 1997; Herbomel *et al.*, 1999; Parichy *et al.*, 2000).

RESULTS

Neutral Red Labels Macrophages in Living Embryos

As long as early macrophages remain in the yolk sac, each of them can be directly visualized and followed at will in the live embryo by DIC video microscopy. This is because the histological structure of the yolk sac is quite simple. The yolk ball is enveloped by two thin cell monolayers, an ectodermal layer, most often designated as epidermis, closely apposed to a protective outer layer, the periderm. Early macrophages wander in the space between the yolk syncitial layer and the epidermis, mostly by creeping on the basal lamina of the latter (Herbomel *et al.*, 1999).

Past the 26-somite stage (22 hpf), the pericardial envelope separates the embryo's head from the yolk sac, so that young macrophages migrating from the yolk sac to the head have to skirt around the pericardium. We could film in live embryos this process of young macrophages migrating on the dorsal aspect of the pericardium to reach the branchial arches (Fig. 1). Such sequences showed that macrophages move individually, some entering branchial ach mesenchyme while others that initially took the very same route end up remaining on the pericardium (Figs. 1B–1F).

To follow the subsequent deployment of early macrophages in the head, we used *in situ* hybridization for the *L-plastin* gene. L-plastin is a leucocyte-specific, cytosolic, actin-bundling protein thought to be involved in the rounding/spreading cycle and motility of all leukocytes in response to signals that activate them (Jones *et al.*, 1998). We showed previously that zebrafish *L-plastin* is expressed in the early macrophage lineage already at the "pre-macrophage" stage, and remains expressed in differentiated, wandering macrophages (Herbomel *et al.*, 1999).

The first few *L-plastin*-positive cells in the head are detected by 22 hpf in the head mesenchyme, most of them still close to the yolk sac (data not shown). Then their number rapidly increases (30 at 24 hpf, 90 at 30 hpf, 180 at 48 hpf) and they spread throughout the head (Figs. 2A–2D).

Correlatively, their number in the yolk sac, which peaked at 160–180 by 30 hpf, decreases to 70–80 by 40 hpf, and down to about 20 by 48 hpf, suggesting that the increasing number of macrophages in the head in the 22- to 48-hpf period is mainly due to their continuing emigration from the yolk sac, together with some local proliferation (see, e.g., Figs. 2K and 4D).

To determine the spatial and temporal patterns of macrophage invasion, we analyzed in detail *L-plastin in situ* hybridized embryos at various developmental stages between 22 and 144 hpf, using both high-resolution DIC microscopy on whole mounts and serial sectioning. To document macrophage behaviors in the invaded tissues, we used DIC video microscopy in live embryos. However, given the complex morphology of the head, we combined DIC video microscopy with vital staining, using neutral red, a classical vital stain for macrophages. Neutral red is taken up through fluid-phase endocytosis and accumulates in the lysosomes of highly endocytic cells—hence in macrophages more than in any other cell type.

We found that neutral red added to the medium readily penetrates all tissues of the live zebrafish embryo or larva. It labels dot-like lysosomes in several cell types, but in a specific pattern in macrophages in which lysosomes appear to fuse with each other into single large, red vacuolar aggregates (Figs. 2H–2J), allowing to detect macrophages easily anywhere in the embryo. Not all macrophages become heavily loaded. In the yolk sac, where all macro-

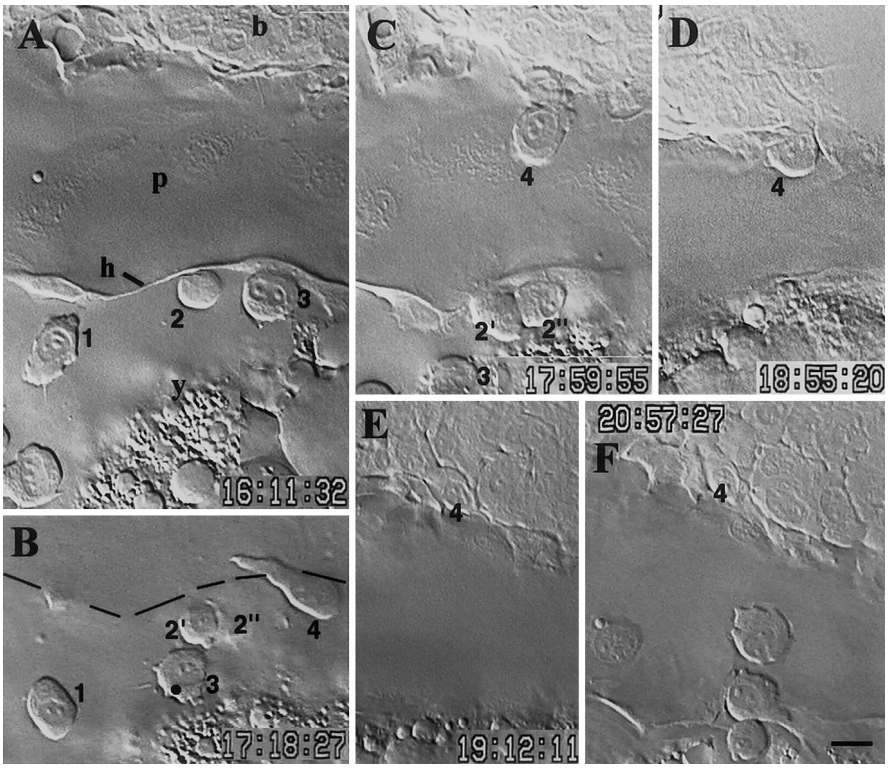

FIG. 1. Early macrophage settling in a branchial arch in the 26- to 30-somite period (22–24 hpf). Sequential lateral views of the same embryo, dorsal upward, rostral to the left. (A) Numbers mark three young macrophages at the lateral border of the pericardial envelope (p), outlined by the pericardial hinge (h, see Fig. 3A in Herbomel *et al.* 1999). (B) Cell 2 divided; a new young macrophage (4) is climbing on the dorsal side of the pericardium. (C) It now reaches the edge of the branchial arch, (D) progressively enters it, (E) and settles there. (F) Fifteen minutes later, two other young macrophages climbed on the dorsal pericardium by the very same route, but then stayed there, becoming residents of the dorsal pericardium. Time indicated in h, min, s; (b) branchial arches, (y) yolk. Bar, 10 μm.

phages can be readily identified by DIC microscopy, one-third to one-half of them do so. Nevertheless, qualitatively, the evolving distribution of macrophages in the embryo revealed by this method is the same as that found by *in situ* hybridization for *L-plastin* gene expression.

Early Macrophages First Invade the Cephalic Mesenchyme

Early macrophages first spread throughout the cephalic mesenchyme. They can be found around the otic vesicles, close to or within the trigeminal ganglion, in branchial arches (Figs. 2K–2N). Many rapidly insert in the narrow spaces between the forebrain and the scleral side of the eyes (Fig. 2E). Others migrate on the hindbrain walls, and some rapidly reach the roof of the fourth ventricle by this route (Figs. 2G and 2M). Most macrophages in the mesenchyme do not appear to contain phagosomes, essentially because apoptosis is scarce at this stage. In the few sites where we found some apoptosis to occur, such as among trigeminal ganglion neurons by 30 hpf, we commonly found a few macrophages phagocytosing apoptotic bodies (Fig. 2N).

Once they have spread throughout the cephalic mesenchyme, early macrophages start colonizing epithelial tissues, a process that requires the ability to cross basal laminae, because these tissues are not vascularized yet. We found that early macrophages first colonize the epidermis, the retinas, and to a lesser extent the various compartments of the brain.

Two Distinct Macrophage Behaviors in the Epidermis

Between 24 and 48 hpf, some of the yolk sac macrophages, most of which were anchored to or spread on the basal lamina of the epidermis, start entering that thin monolayered epithelium. They intercalate between epidermal cells, and once there, they adopt one of two behaviors. Some stay in a quiescent, highly digitated form (Figs. 3A and 3B). Others restlessly wander in that thin cell layer, showing their overwhelming ability to deform their overall shape and nucleus to literally flow inbetween epidermal cells (Figs. 3C–3H, and movie 1; URL for viewing the accompanying movies: http://www-alt.pasteur.fr/

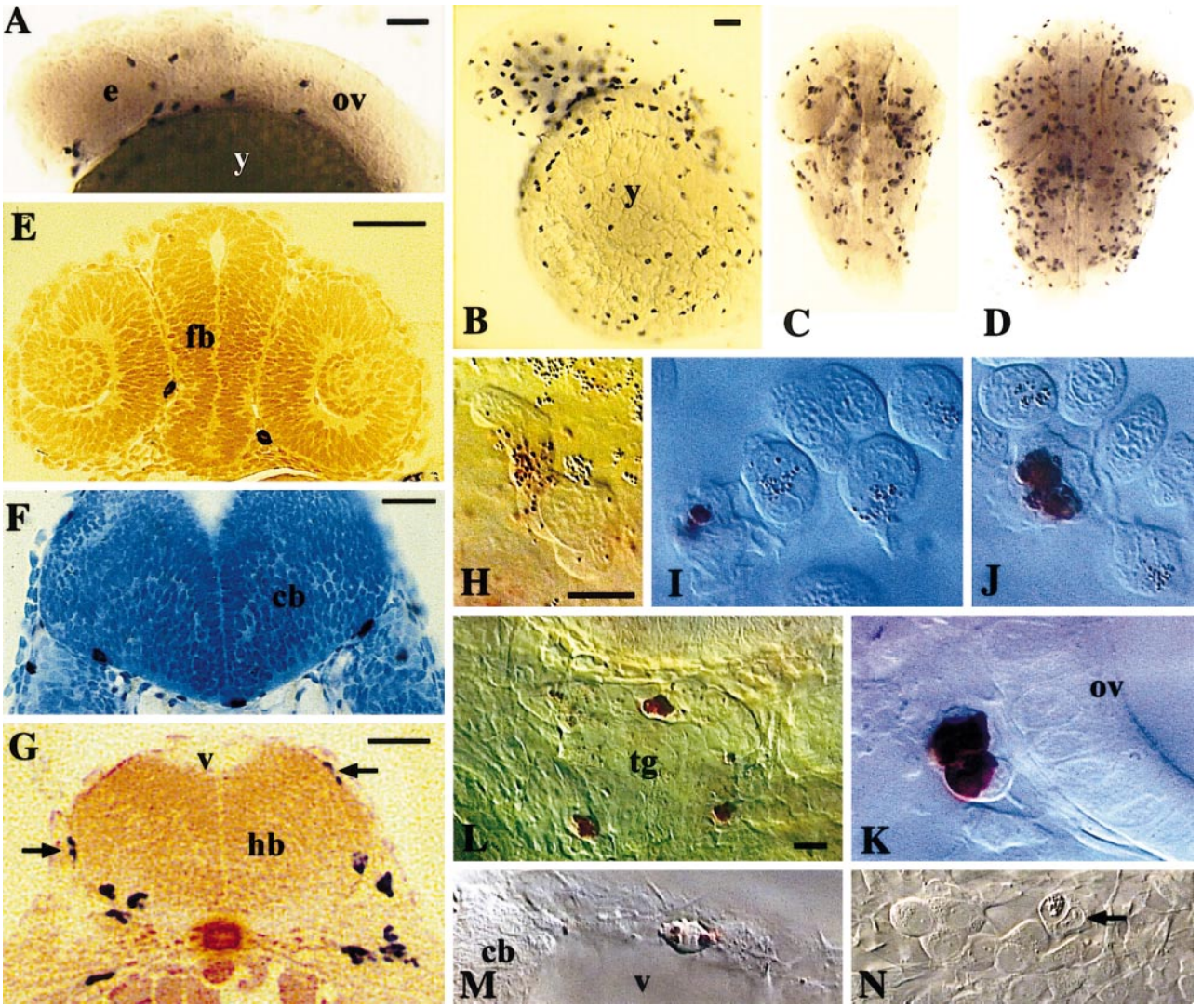

FIG. 2. Rapid spreading of early macrophages throughout the head. (A–G) *In situ* hybridization for *L-plastin*. (A) Lateral view of the head, 25 hpf. (B) Lateral view of the head and yolk sac, 35 hpf. (C, D) Dorsal views of the head at 35 hpf (C) and 48 hpf (D). (E–G) Cross sections; (E) 25 hpf; two macrophages in the interstices between eyes and forebrain (fb); (F) 35 hpf; three macrophages adhering to the ventral basal lamina of the cerebellum anlage (cb); (G) 35 hpf; macrophages caudal to the otic vesicle, migrating on the hindbrain walls (arrows) and inside the hindbrain ventrally. (H–N) Live embryos at 28–35 hpf viewed by DIC combined with neutral red staining (H–M), or by DIC alone (N); lateral views, dorsal up, anterior to the left. (H–J) Macrophages in the yolk sac blood circulation valley, showing the progression of the neutral red staining process (see text); cells with no stained lysosomes are erythroblasts. (K) Two probably sister macrophage cells adjacent to the otic vesicle. (L) Three macrophages associated with the trigeminal ganglion (tg). (M) Macrophage wandering on the roof of the fourth brain ventricle (v). (N) Phagocytic macrophage (arrow) among trigeminal ganglion neurons. (y) yolk sac; (e) eye; (ov) otic vesicle; (fb) forebrain; (hb) hindbrain; (cb) cerebellum anlage; (tg) trigeminal ganglion; (v) fourth brain ventricle. Bars: (A) 50 μm; (B–D) 50 μm; (E) 50 μm; (F, G) 25 μm; (H–K) 10 μm; (L–N) 10 μm.

~herbomel/). Quite strikingly, the most common trajectory that we observed in our video time-lapse sequences was a macrophage wandering all the way round an epidermal cell, in 2–10 min, according to the size of the epidermal cell (Figs. 3E–3H, and movie 1).

Unlike the other colonization processes described in this paper, the onset and extent of macrophage colonization of the yolk sac epidermis is highly variable among embryos. The most typical time window is between 30 and 36 hpf, but in some embryos, it can start as early as 22 hpf, and in others not before hatching (50 hpf). *In situ* hybridization as well as direct observation of live embryos revealed that early macrophages also colonize the epidermis of the embryo's head, and display there the same swift motility and

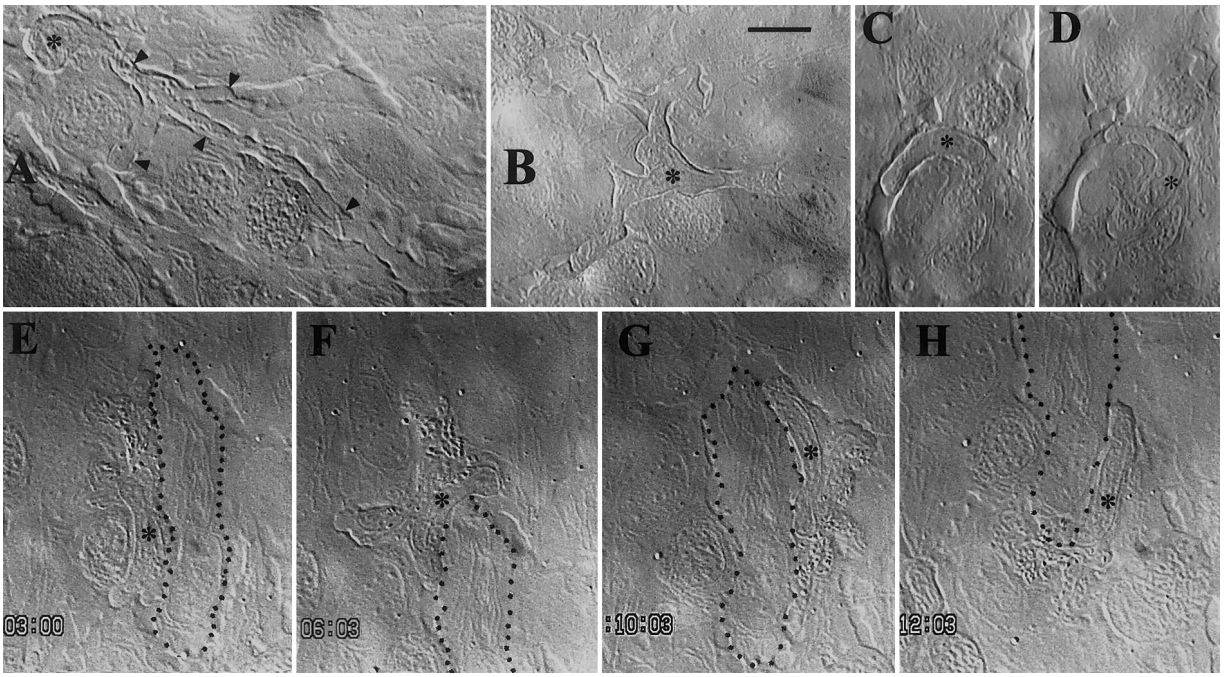

FIG. 3. Early macrophages in the yolk sac epidermis. Asterisks mark macrophage nuclei. Filaments inside cells are mitochondria. (A, B) 30 hpf; macrophages of the still type, interdigitating (black arrowheads in A) between epidermal cells. (C, D) 30 hpf; macrophage wandering round a small epidermal cell; (D) is 80 s after (C). (E–H) 48 hpf; macrophage wandering all the way round a long epidermal cell (dotted contour) in 12 min. Time indicated in min, s. Bar, 10 μm.

characteristic trajectories around epidermal cells as in the yolk sac epidermis (data not shown).

Thus, video time-lapse sequences show here again the individual nature of macrophage behavior in a given tissue, and the occurrence of two contrasted types in the epidermis.

Nose and Neuromasts

Among sensory organs derived from epidermal placodes, we found that several macrophages associate with the olfactory placodes, such that by 50 hpf they are arranged in a circle around the base of each placode (Figs. 4A and 4B), and later also often found inside the olfactory epithelium (Fig. 4C).

Macrophages also arrange in circles around neuromasts of the anterior lateral line, but only starting at 4–5 dpf (Figs. 4D–4F). In fact, at that stage and later, virtually all macrophages in the dorsal epidermis of the head are associated with neuromasts. We found macrophages similarly associating with neuromasts of the posterior lateral line all along the trunk and tail.

Retina

By 26–30 hpf, one to three macrophages can be seen in the vitreous space and choroid fissure of every embryo (Figs.

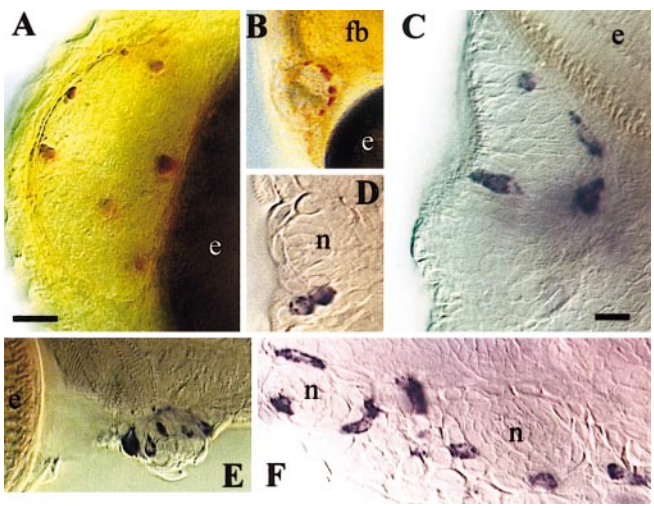

FIG. 4. Early macrophages around olfactory organs and neuromasts. (A, B) Neutral red vital staining of macrophages associated with the left olfactory organ at 50 (A) and 84 hpf (B, low magnification). (C–F) *In situ* hybridization for *L-plastin*; (C) Right olfactory organ, 96 hpf, dorsal view. (D) Two macrophages, probably sister cells from a recent mitosis, adjacent to an anterior neuromast at 120 hpf. (E) A latero-ventral neuromast just caudal to the eye at 120 hpf. (F) Two neuromasts of the supra-orbital line at 144 hpf. (fb) forebrain; (e) eye; (n) neuromast. Bars: (A) 20 μm; (C–F) 10 μm.

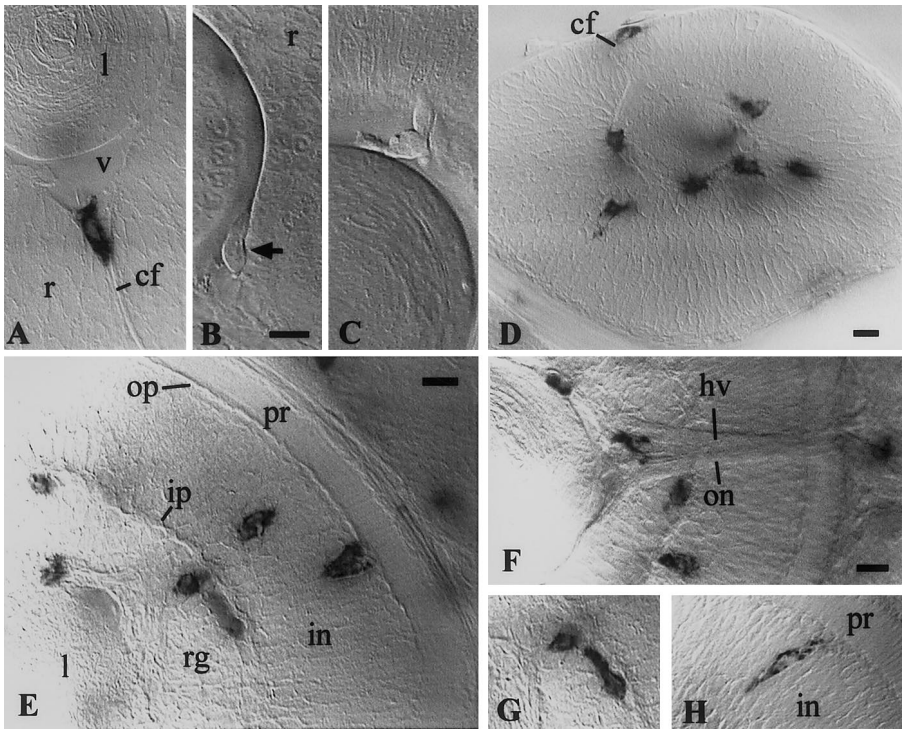

FIG. 5. Early macrophages in the retina. (A, D–H) *In situ* hybridization for *L-plastin*. (B, C) Live embryos, 30 hpf. (A, B) macrophage in the choroid fissure, entering the vitreous space, between lens and retina, at 26 (A) and 30 hpf (B). (C) macrophage already in the vitreous space. (D) 35 hpf; macrophages have invaded the vitreous-proximal part of the retina; one is appearing in the choroid fissure. (E–G) 48 hpf; the macrophage lying tangentially along the inner plexiform layer in (E) is shown in focus in (G); (H) 72 hpf. (v) vitreous space; (l) lens; (r) retina; (pr):photoreceptor cell layer; (op) outer plexiform layer; (in) inner nuclear layer; (ip) inner plexiform layer; (rg) retinal ganglion cell layer; (cf) choroid fissure; (on) optic nerve; (hv) hyaloid vein. Bars, 10 μm.

5A–5C). A significant colonization of all retinas occurs by 35 hpf. Each retina contains 3–12 L-plastin-positive cells, most of them close to or in contact with the vitreal surface (Fig. 5D). At 48 hpf and later, there are 30–35 macrophages per retina. The retinal cell layers have now differentiated, and the macrophages are found at all depths in the retinal ganglion cell layer and inner nuclear layer (Figs. 5E–5H, and movie 3). They appear to be excluded from the photoreceptor cell layer, as well as from the plexiform layers. Some of them are stretching radially, with one of their ends abutting the distal or proximal limit of the cell layer in which they are inserted. Others stretch tangentially along the inner plexiform layer (Fig. 5G). No macrophage was found to stretch across the inner plexiform layer.

We never found any macrophage in the lens, although by 24–30 hpf it is the only site of extensive apoptosis in the embryo.

Brain

When macrophages invaded the head mesenchyme in the 23- to 30-hpf period, several were quickly found in close contact with brain boundaries, adhering to the pial surface of all brain compartments, and on the roof of the fourth ventricle (Figs. 2F, 2G, and 2M). From about 35 hpf onwards, the fourth ventricle contained two to four macrophages, initially in a strikingly stereotyped, posterior location—dorsal to the first two somites (Fig. 6A). We never found any macrophage in the other, more rostral brain ventricles.

We found that colonization of the brain itself slowly starts by 35 hpf, apparently anywhere among brain compartments, but in low cell numbers (Fig. 6). Despite the inherent difficulty of tracking macrophage movement in a dense three-dimensional tissue, an extensive series of time-lapse DIC video recordings enabled us to catch brain macrophages whose wandering remained for 30 min in the focal plane. One is shown here in movie 2, with selected frames in Figs. 6B–6D. The surprising feature is the speed at which macrophages are able to wander in the so dense neuroepithelium.

At 48 hpf, the forebrain, midbrain, and hindbrain each contained 5–10 L-plastin-positive cells. We found them anywhere inside the neuroepithelium, main longitudinal axonal tracts, and commissures (Figs. 6F–6J). One virtually constant feature was the association of three to six macro-

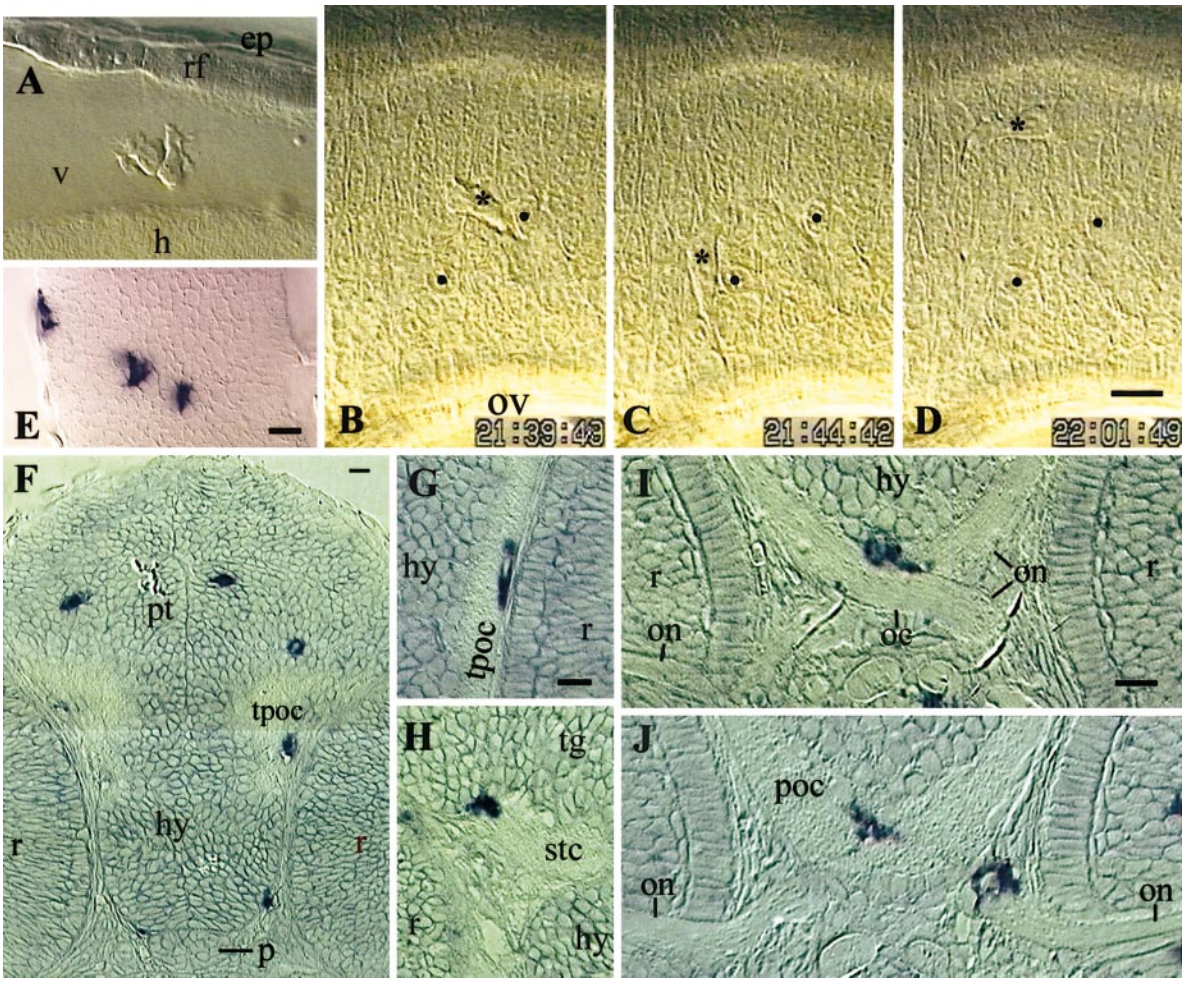

FIG. 6. Early macrophages in the brain. (A–D) Live embryos, 35 hpf, lateral view, rostral to the left. (A) Two macrophages in the fourth brain ventricle, dorsal to the first somite. (B–D) Three instants of the macrophage wandering in hindbrain rhombomere 5 (shown in movie 2; asterisk, macrophage nucleus; two neuroepithelial cell nuclei labeled by black dots serve as reference points; time indicated in h, min,s. (E–J) *In situ* hybridization for *L-plastin*. (E) 35 hpf, hindbrain, left half, dorsal view, rostral upward. (F–J) Resin cross sections, 48 hpf. (F) Section through the pretectum (pt), hypothalamus, and pituitary (p). (G) Macrophage in the tract of the post-optic commissure (TPOC). (H) Macrophage partly in the tegmentum (tg), partly in the sub-tegmental commissure (stc). (I, J) Two successive sections, in rostro-caudal order, showing one macrophage bridging the optic chiasm (oc) and post-optic commissure (poc) (I, J), and another one in the mesenchyme, riding on the optic nerve (J). (h) hindbrain wall; (v) fourth ventricle; (rf) roof of the fourth ventricle; (ep) epidermis; (ov) otic vesicle, (hy) hypothalamus, (tpoc) TPOC, (r) retina, (on) optic nerves. Bars, 10 μm.

phages with the optic tracts, typically at or close to the optic chiasm, and in the mesenchyme, adhering to the short optic nerves (Figs. 6I and 6J).

By 60 hpf, the number of macrophages started to increase specifically in the midbrain optic tectum (Fig. 7A, and see below).

A Phenotypic Transition to "Early Microglia"

By 60 hpf, the *L-plastin in situ* hybridization signal in all brain and retinal macrophages starts decreasing (Fig. 7A), relative to macrophages anywhere else in the embryo, so that by 96 hpf, only very faint L-plastin signals can be detected in these regions. Yet, vital staining with neutral red reveals that the macrophages are still there, but appear to have undergone a phenotypic transition, part of which consists in extinction of L-plastin expression.

Before 55 hpf, only one-third to one-half of *L-plastin*-positive cells in the brain and retina were vitally stained by neutral red, as in the rest of the embryo. At 55–60 hpf, this changes radically. The numbers indicate that all *L-plastin*-positive cells in the brain and eyes are now stained by neutral red, and their staining is so heavy (Figs. 7B–7D) that they are readily seen individually under the dissecting

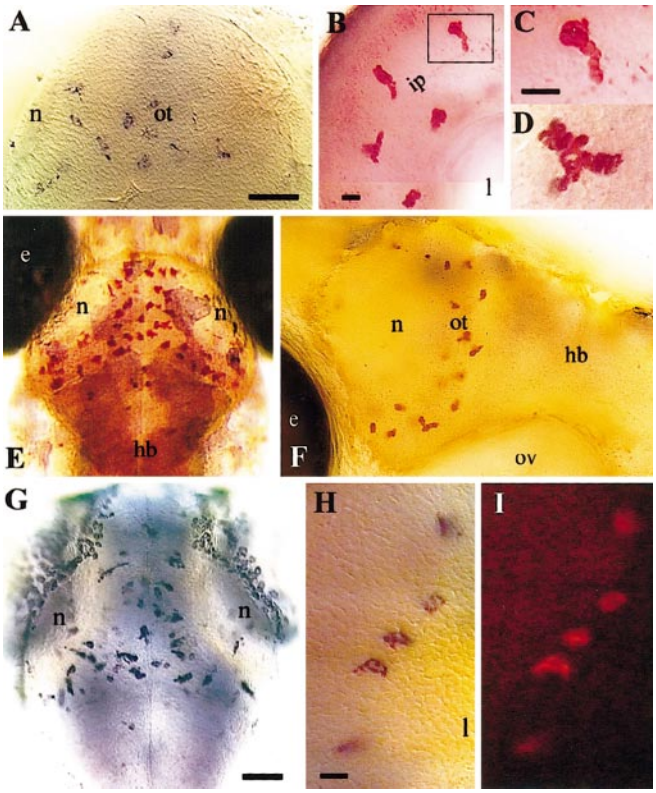

FIG. 7. Phenotypic transition of brain and retinal macrophages to early microglia; colonization of the optic tectum. (A, E, G) Dorsal view of the optic tectum, rostral upward. (A) 60 hpf, *L-plastin in situ* hybridization. (B–F) Neutral red-stained live embryos. (B) Retina, 65 hpf; the boxed early microglial cell is shown at higher magnification in (C). (D) Optic tectum, 82 hpf. (E, F) 99 hpf; (F) lateral view showing the extent of the left tectal neuropile, (G) *In situ* hybridization for *apoE*, 72 hpf. (H, I) Retina, 72 hpf; double *in situ* hybridization for *L-plastin* (blue) and *apoE* (red), (I) showing the red fluorescence of the *apoE* signal. (hb) hindbrain; (ot) optic tectum; (n) tectal neuropile; (e) eye; (ip) inner plexiform layer; (l) lens; (ov) otic vesicle. Bars: (A) 50 μm; (B) 10 μm; (C, D) 10 μm; (G) 50 μm; (H, I) 10 μm.

scope (see Figs. 7E and 9K), a series of coalescent neutral red-filled large vesicles roughly delineating the shape of each cell (Figs. 7C and 7D).

Neutral red staining revealed that the specific colonization of the optic tectum detected at 60–72 hpf by *L-plastin in situ* hybridization actually continued until 50–60 cells were there at 84–96 hpf, evenly distributed in the tectum, but strictly excluded from the tectal neuropiles (Figs. 7E and 7F). At 7.5 dpf, they were still there.

The distribution and kinetics of appearance of these highly endocytic cells in the optic tectum, retina, and forebrain was quite reminiscent of the expression pattern of the *apolipoprotein E* (*apoE*) gene (Babin *et al.*, 1997). A closer look confirmed the parallelism: at 72 hpf and later, *apoE* is expressed in large, irregularly shaped cells in the optic tectum, strictly excluding the bilateral neuropiles (Fig. 7G), and in the retina in a pattern similar to the L-plastin-positive cells a day earlier.

Therefore. we performed a double *in situ* hybridization experiment for *L-plastin* and *apoE* at 72 hpf. This experiment revealed a 100% coincidence of weakly *L-plastin*-positive and strongly *apoE*-positive cells in the brain and retina (Figs. 7H and 7I). In contrast, no *L-plastin*-positive cell outside the brain was found to be *apoE*-positive.

Because all retinal and brain macrophages, and only they, undergo the phenotypic transition just described, we decided to call the resulting cells "early microglia."

Beside early microglia, neutral red staining revealed one other population of 20–25 highly endocytic (but *apoE*-negative) macrophages ventrally, just rostral to the heart, and only between 72 and 84 hpf (see Fig. 9K). We found that these highly endocytic macrophages are actually associated with the regression of the hatching gland that occurs precisely during this time interval (P.H., unpublished data).

M-CSF Receptor Function Is Required for Macrophage Invasion

The *panther* mutation is a loss-of-function mutation of a zebrafish orthologue of *fms*, coding for the macrophage colony-stimulating factor (M-CSF, also known as CSF-1) receptor, that hinders the development of yellow pigment cells, called xanthophores (Parichy *et al.*, 2000). Zebrafish *fms* is expressed in neural crest precursors of xanthophores, is required for their ventralward migration and differentiation, and was also mentionned to be expressed in macrophage progenitors (Parichy *et al.*, 2000).

We reexamined *fms* expression at various stages of development and investigated whether the *panther* mutation would affect the deployment and behaviors of early macrophages in the embryo.

We found that *fms* is already expressed in the early macrophage lineage at 22 somites, i.e., among "pre-macrophages" maturing in the yolk sac, and then remains expressed in all tissue macrophage populations described in this paper, including early microglia (Fig. 8). In the *panther*^{i4blue} mutant, *fms* expression was undetectable.

As far as we can tell from our high-resolution DIC time-lapse video recordings, early macrophages in *panther*^{i4blue} initially behave as wild type. Pre- and young macrophages accumulate under the hatching gland and along the pericardium, some of them migrating on its dorsal side towards branchial arches, as wild type in Fig. 1. They divide actively, and spread in the yolk sac (Figs. 9A, 9B, and 9E). When erythroblasts arrive in the yolk sac, the young macrophages interact with them and phagocytose their apoptotic bodies (Fig. 9C). They are vitally stained by neutral red as wild-type cells (Fig. 9D).

But then *panther* macrophages totally fail to emigrate from the yolk sac and pericardial area to colonize embryonic tissues. At 36 hpf, when wild-type embryos already have nearly 100 macrophages in their head, *panther* mu-

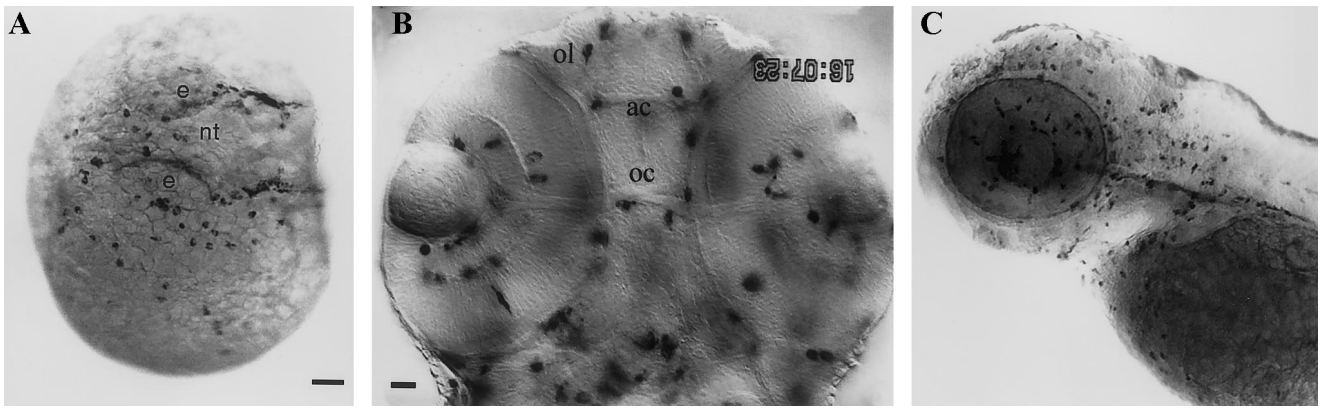

FIG. 8. Expression of the *fms* gene in the early macrophage lineage. (A) 25-somite (21.5 hpf), dorso-lateral view; beside pre-/young macrophages spread on the yolkball, *fms*-positive xanthophore precursors outline the lateral borders of the neural tube (nt); (e) eye. (B) 48 hpf, head, deep dorsal view. Out-of-focus *fms*-positive macrophages produce the multiple shadows. (ol) olfactory organ; (ac) anterior commissure; (oc) optic chiasm. (C) 72 hpf, lateral view. Bars: (A, C) 50 μm; (B) 20 μm.

tants only have a few individuals on the scleral surface and/or at the caudal border of the eyes (Fig. 9E). No macrophage penetrates the retina, brain, or epidermis—even in the yolk sac. At 44 and 56 hpf, we counted about 35 macrophages in the head, but close inspection revealed that most actually were in blood vessels (Figs. 9F and 9G). In the yolk sac, outside the bloodflow there were few L-plastin-positive cells left, indicating that most probably, early macrophages were progressively taken away by the blood-flow into the vasculature. In the next 2 days, early macrophages were found essentially in the ventral head (eye muscles, jaw, and gills), pericardial area, and blood circulation (Fig. 9H). At 72 hpf, they did not invade the regressing hatching gland, nor did they massively colonize the optic tectum (Figs. 9I–9K). However, a mean number of three macrophages (0–7/embryo) did penetrate the optic tectum. They were stained heavily with neutral red and showed strong *apoE* expression, i.e., they had differentiated in early microglia. Then colonization of the optic tectum eventually occured in the majority of *panther* embryos over the next 4 days (Figs. 9L–9N). It leveled off at 20–24 cells/tectum, a number reached by 1/3 of embryos at 5.5 dpf, and 2/3 at 7.5 days, with microglial cells arranged as in the wild-type—evenly spaced but excluded from the tectal neuropiles (Figs. 9M and 9N). The other brain compartments also became colonized with the same kinetics, in the same small proportion relative to optic tectum as in wild type. At 7.5 days and not before, some retinas also became colonized, by 12–25 microglial cells (not shown).

Between 66 hpf and the actual, delayed microglial colonization of these tissues, vast numbers of apoptotic bodies accumulated throughout the optic tectum and retina (Figs. 10A–10C). When macrophages finally arrived in the tissue, they phagocytosed large numbers of these corpses (Figs. 10D–10F). Several hours after the 20–25 microglial cells had settled in the optic tectum, most apoptotic bodies had disappeared.

DISCUSSION

After having identified the origin of early macrophages (Herbomel *et al.*, 1999), we now analyze their colonization of embryonic tissues and their differentiation in early microglia. Figure 11 summarizes our results.

We first see a massive invasion of the cephalic mesenchyme, starting by 22–23 hpf, about 5 h before it becomes vascularized. As a result, by 30 hpf and later, no anatomical structure in the head of the zebrafish embryo is farther than a few micrometers from some macrophages. Then, as in mammals and birds (Sorokin *et al.*, 1992a; Cuadros *et al.*, 1993), the retina and brain start to be colonized. So does the embryonic epidermis. The retina and epidermis are avascular, and the brain starts becoming vascularized only several hours after the onset of its colonization (Isogai *et al.*, 2001, and our unpublished data). Thus, in contrast with the classical view (see references in Sorokin *et al.*, 1992b), these tissues do not receive their first resident macrophages through the blood, as circulating monocytes extravasating from blood vessels, but through an invasive process that must involve the crossing of brain, retinal, and epidermal basal laminae by cells of the early macrophage lineage. As regards the retina, the invasion route is clear: from the mesenchyme, early macrophages reach the vitreous space through the choroid fissure. They enter the retina at its vitreal side, and from there spread to deeper, more scleral levels. The same route was concluded by studies in mammals and birds (Ashwell, 1989; Ashwell *et al.*, 1989; Cuadros *et al.*, 1991). Concerning the brain, the paths of invasion are more elusive. We found macrophages adhering to the pial surfaces of the brain and to the roof of the fourth

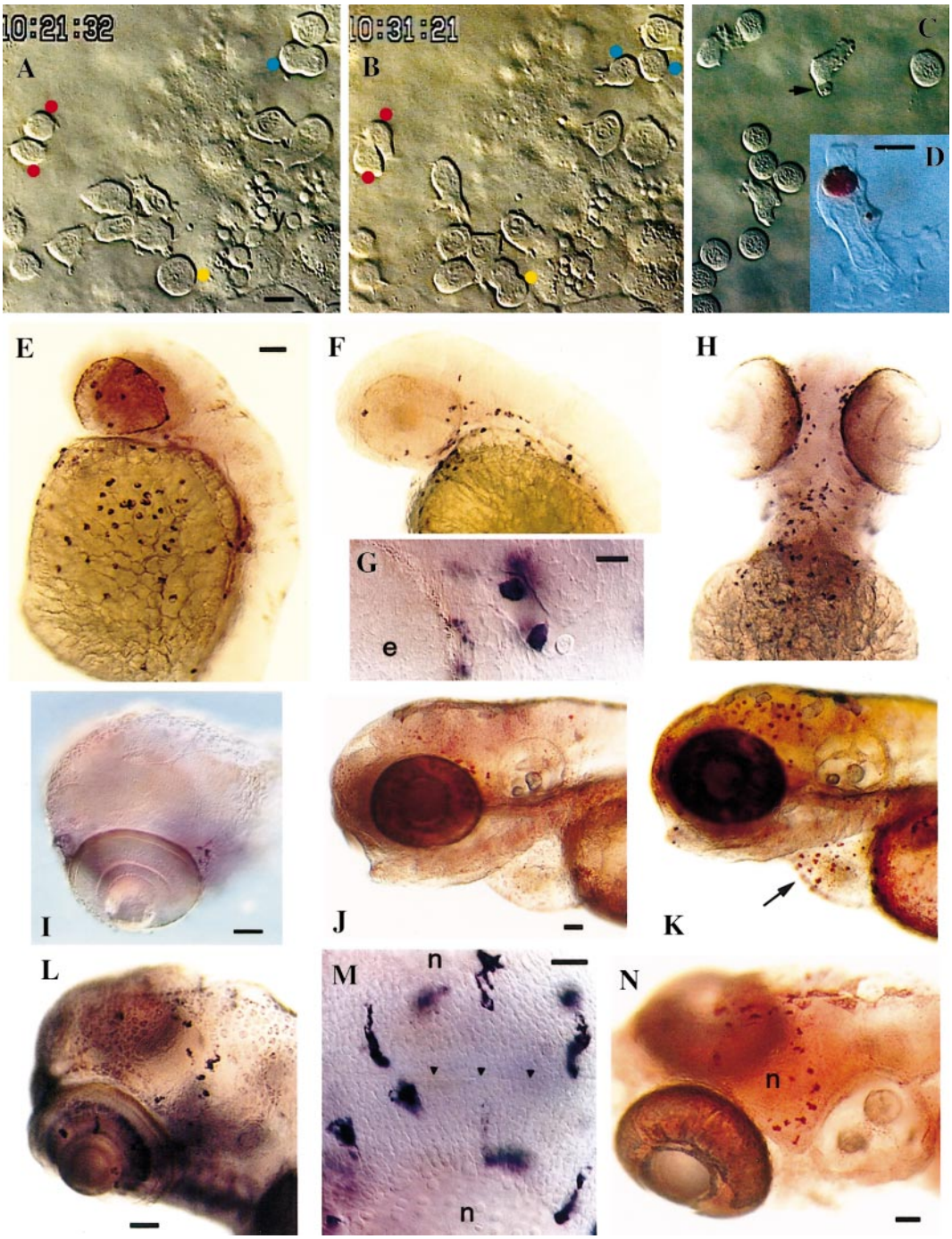

FIG. 9. Behavior of early macrophages in the *panther* mutant. All *panther* embryos, except K. (A–D) Live recordings of early macrophage behaviors in the yolk sac. (A, B) 26-somite stage (22 hpf). (A) Red dots mark sister cells from a mitosis that occured 15 min earlier; two other cells are presently in mitosis: the blue-dotted cell in anaphase B, the yellow-dotted one in pro-metaphase. (B) Ten minutes later, the blue-dotted cell cleaved in two daughter cells; the yellow-dotted cell is in anaphase. (C) 25 hpf; erythroblasts (rounded cells) have now joined the yolk sac and macrophages interact with them; one is phagocytosing an apoptotic residue (arrow). (D) 25 hpf, neutral red staining. (E–H) *In situ* hybridization for *L-plastin*. (E, F) Lateral views at 36 hpf (E; compare with wt in Fig. 2B) and 44 hpf (F). (G) 44 hpf, dorsal view, anterior to the left; two positive cells in a cephalic vessel. (H) 72 hpf, ventral view. (I, L) *In situ* hybridization for *apoE* at 72 hpf (I; compare with wild-type in Fig.7G) and 132 hpf (L); (J, K) 72 hpf; neutral red staining of live *panther* (J) and wild-type (K) embryos, showing macrophages associated with the optic tectum and regressing hatching gland (arrow). (M) 132 hpf; *in situ* hybridization for *apoE*, optic tectum, dorsal view, rostral to the left; (arrowheads) midline. (N) 7.5 days, neutral red staining (compare with wild-type at 99 hpf in Fig. 7F). (n) tectal neuropile. Bars: (A–C) 10 μm; (D) 5 μm; (E, F, H) 50 μm; (G) 10 μm; (I) 50 μm; (J, K) 50 μm; (L) 50 μm; (M) 20 μm; (N) 50 μm.

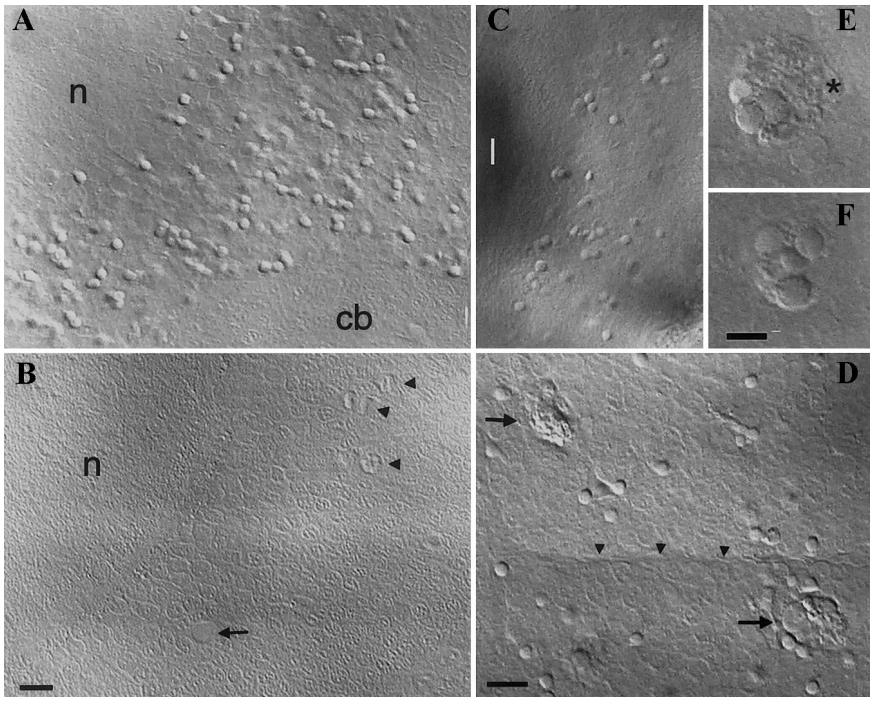

FIG. 10. Apoptotic bodies accumulate in *panther* optic tectum and retina until eventual microglial colonization. Live embryos, 120 hpf, DIC optics. (A, B) Optic tectum, dorsal view, rostral upward, (A) *Panther* embryo. (B) Wild-type embryo; yellow shadows are due to xanthophores present above the brain (absent in *panther*); (arrow) blood vessel; (arrowheads) mitotic cells. (C) Retina. (D) Newly arrived early microglial cells (arrows) eliminating apoptotic bodies in the optic tectum; (arrowheads) midline. (E, F) Close-up on a tectal phagocyte at two depth planes, showing 7 still recognizable apoptotic bodies within its phagocytosed material; (asterisk) macrophage nucleus. (cb) cerebellum, (n) tectal neuropile. Bars: (A–C) 10 μm; (D) 10 μm; (E, F) 5 μm.

ventricle, and then simultaneously in the fourth ventricle and in the neuroepithelium, suggesting that they enter the brain by these two routes—which mammalian and avian studies also suggested.

Beyond these common features, we find specific differences in the zebrafish embryo. First, early macrophage invasion is more strictly confined to the head tissues. Outside the circulatory system and surrounding mesenchyme, and neuromasts after 4 dpf, we found virtually no macrophages in the trunk and tail. In rodents and birds, although the head mesenchyme and brain were colonized first, early macrophages then also spread to some extent in the rest of the body, notably colonizing the spinal chord in a rostro-caudal sequence (Sorokin *et al.*, 1992a; Cuadros *et al.*, 1993). In zebrafish embryos examined up to 7 dpf, we never found any macrophage in the spinal chord, even though macrophages were often found in the posteriormost part of the hindbrain.

Dynamic Aspects of Macrophage Behavior in Embryonic Tissues

Thanks to DIC video microscopy, our present study provides access for the first time to the dynamics of macrophage wandering in the tissues of a live vertebrate. In the embryonic epidermis, this revealed two contrasting behaviors: macrophages staying still, spread dendritically inbetween epidermal cells; and fast wandering ones. The dendritic shape of the still macrophages is reminiscent of dendritic cells of the skin in mammals, i.e., Langerhans cells. Mizoguchi *et al.* (1992) actually provided evidence that in the mouse, Langerhans cells may originate from the early macrophage lineage, and we will investigate this possibility in the zebrafish.

Macrophages freshly arrived in the brain also showed a surprisingly swift wandering in such a dense tissue. The video sequences show them covering a distance equivalent to the dorso-ventral extension of a rhombomere in about 15 min. One important consequence is that a small number of such macrophages would be sufficient to cover the whole brain in a short time, e.g., sampling/probing brain cells and interstitial medium, and/or distributing signalling, trophic, or ECM-remodeling molecules accordingly. The same prospect applies to epidermal macrophages.

So far, the movement of macrophages in vertebrate tissues was always considered and studied in the context of inflammation, and towards inflammatory foci (Florey, 1968). Our present data suggest that tissue macrophages

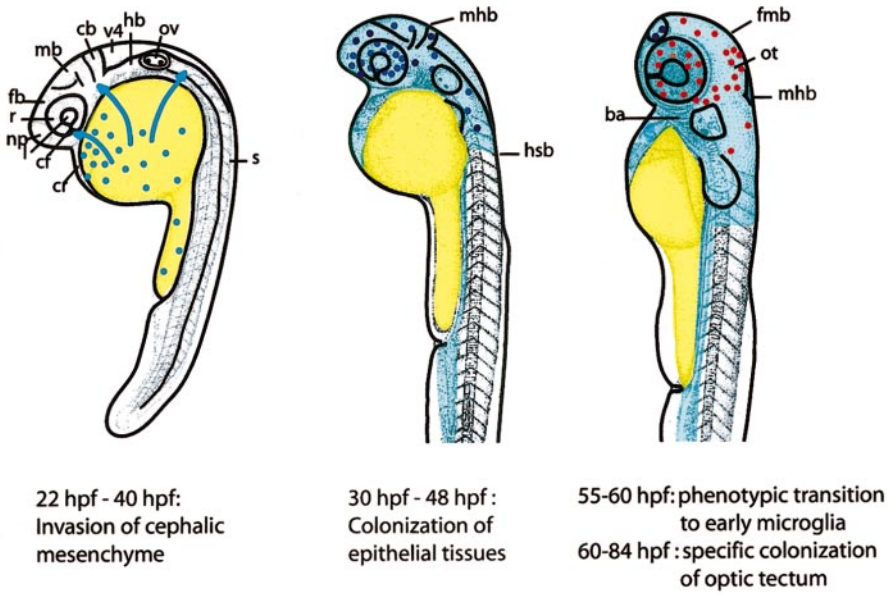

FIG. 11. Spatial and temporal deployment of early macrophages in the zebrafish embryo. The yolkball is in yellow. Left embryo: light blue arrows represent the emigration of early macrophages (light blue dots) from the yolk sac to embryonic tissues. Middle embryo: light blue shading indicates the extent of embryonic mesenchyme colonized by early macrophages; dark blue dots represent macrophage colonization of epithelial tissues—brain, retina, and olfactory placode. For the sake of clarity, colonization of the epidermis is not represented. Right embryo: red dots represent early microglial cells in the brain and retina. (cr) cardiac region; (cf) choroid fissure; (l) lens; (r) retina; (np) nasal placode; (fb) forebrain; (mb) midbrain; (hb) hindbrain; (cb) cerebellum anlage; (v4) fourth brain ventricle; (ov) otic vesicle; (s) spinal chord; (fmb) forebrain–midbrain boundary; (mhb) midbrain/hindbrain boundary; (hsb) hindbrain–spine boundary; (av) axial vein; (ba) branchial arches.

may be restlessly wandering in their tissue of residence at steady state, in the healthy organism. We propose that such a behavior represents macrophage patrolling, for immune, and possibly also developmental and trophic surveillance. Patrolling would be one of two ways to achieve such surveillance, the other way being a network of relatively static, evenly spaced and ramified cells—a strategy typically embodied in adult mammals by ramified microglia in the brain or Langerhans cells in the skin.

Zebrafish Early Macrophages and the Visual Pathways

Unlike their mammalian and avian homologues, zebrafish early macrophages colonize the retina and optic tectum much more heavily than the rest of the brain. The heavy colonization of the tectum results from a distinct wave occuring about 30 h later than the primary, low-level colonization of the brain. By this stage, the whole brain is well vascularized and therefore, in contrast with the primary wave, we cannot tell so far whether these new residents of the tectum invaded it by crossing its basal lamina or by extravasating from blood vessels irrigating it.

In the retina, as the retinal cell layers differentiate, early macrophages appear to avoid entering the inner plexiform layer (IPL)—in contrast with the retinal microglia of adult vertebrates, including fish (Dowding *et al.*, 1991; Velasco *et al.*, 1999). However many adhere to the IPL, sometimes even stretching along it tangentially. Thus the IPL seems to represent for them a physical barrier, to which they can adhere, rather than an area from which they are chemically repelled. Similarly, macrophages/early microglia invading the optic tectum are completely excluded from the tectal neuropiles, but are frequently found adhering to the neuropile border. The plexiform layers and tectal neuropiles are the main sites of synaptic connections in the retina and optic tectum, respectively. The first synapses appear at 60 hpf in the IPL (Schmitt and Dowling, 1999), and probably by 65–70 hpf in the tectal neuropile (Easter and Nicola, 1996; Kaethner and Stuermer, 1997). Thus, in both cases, early macrophages appear specifically excluded from regions of synaptogenesis, already before the first synapses form. We surmise that their presence is not wellcome where delicate dendritic and axonal arborizations are developing, and soon elaborating synaptic contacts.

Why do zebrafish early macrophages/microglia colonize mainly the retina and optic tectum? Fish brain and retina grow continuously through life. But while the retina grows by new annuli added peripherally (as a tree trunk), the optic tectum grows by adding crescents posteriorly. The mainte-

nance of retinotopy is achieved by a continuous rewiring of retino-tectal projections, a process in which axons retract their terminals from previous locations and re-arborize in new, adjacent areas (Easter, 1986). This process of continually "shifting terminals," which is thought to occur since the beginning (S. Easter, personal communication), is likely to require a steady membrane lipid supply, through the apoE carrier, as synaptic remodeling does in the mammalian brain (see below). This could justify the numerous tectal microglia, and retinal microglia could also contribute by providing apoE-borne lipids to the cell bodies of ganglion neurons.

Transformation of Early Brain and Retinal Macrophages in "Early Microglia"

This phenotypic transformation affects all brain and retinal macrophages simultaneously at 55–60 hpf, regardless of how much time each of these cells has already spent in that tissue. Moreover, new macrophages that enter the brain past 60 hpf, e.g., to colonize the optic tectum, or in response to brain wounding (our unpublished results), must undergo this transformation right away, because we then see no brain macrophage other than with the early microglial phenotype. In this phenotypic transition, macrophages adopt more irregular shapes, they become very highly endocytic, they reduce their expression of L-plastin, and they abruptly start to express apoliprotein E at a high level.

The high level of endocytic activity might serve for the cleansing of the brain interstitial fluid, in which all kinds of neurotransmitters are continuously released (Ward *et al.*, 1991), especially since there are no astrocytes in the fish to take up this role (see below).

Apolipoprotein E is considered a neurotrophic factor in the mammalian brain, where it is probably the main lipid carrier (Poirier, 1994), as well as a facultative dimerization partner of ciliary neurotrophic factor that potentiates its neurotrophic effects (Gutman *et al.*, 1997). In adult mammals, ApoE is a major secretion product of various macrophage populations (Werb and Chin, 1983; Hashimoto *et al.*, 1999). Yet in the brain, astrocytes are the main source of apoE (Boyles *et al.*, 1985). Upon peripheral nerve regeneration, apoE is strongly induced in macrophages gathering at the site of lesion. In the brain, synaptic remodeling is also associated with local induction of apoE secretion, now by astrocytes (Poirier, 1994). In fact, astrocytes of mammals appear to have at least partially taken up several other traditional functions of macrophages, such as antigen presentation, phagocytosis (of myelin processes), or fluid cleansing (Soos *et al.*, 1998; Burudi *et al.*, 1999; Bechmann and Nitsch, 2000). This quite probably goes along with the down-regulation of many macrophage-specific functions in the so-called "ramified" or "resting" microglia of adult mammals and birds. Ontogenetically, both astrocytes and ramified microglia appear late, around birth and later, astrocytes arising from the transformation of embryonic radial glia (Misson *et al.*, 1991), and then ramified microglia from the transformation of embryonic/perinatal amoeboid (i.e., macrophage-like) microglia (Giulian and Baker, 1986). Phylogenetically, astrocytes and ramified microglia are also recent. In the adult fish brain, radial glia remain through life, and true (stellate) astrocytes are not found (Kalman, 1998). In contrast, microglia appears much more numerous than in mammals, and is of the amoeboid type (Dowding and Scholes, 1993), as the zebrafish early microglia described here.

We therefore suggest that in lower vertebrate embryos and adults as well as in amniote embryos, amoeboid microglia assumes not only immune, but also fluid cleansing and trophic functions, among which apoE secretion, as well as probably other functions usually ascribed to astrocytes in adult mammals.

The M-CSF Receptor Is Essential for Early Macrophage Deployment in Embryonic Tissues

Macrophages are most commonly thought of as scavengers, in charge of eliminating apoptotic bodies. However, apoptosis is scarce in zebrafish embryonic tissues by the time early macrophages colonize them. Therefore, although we found that zebrafish early macrophages do their scavenging job locally once they have invaded a given tissue, their overall pattern of invasion of the mesenchyme and forming organs in the wild-type embryo cannot be due to their attraction by apoptotic cells. Similar conclusions were drawn for early macrophages of mammals and birds (Ashwell, 1989, 1991; Sorokin *et al.*, 1992a; Cuadros *et al.*, 1993).

We found that *fms*, a zebrafish M-CSF receptor gene orthologue, is expressed in all cells of the early macrophage lineage, and is crucial for their colonization of embryonic tissues. Lichanska *et al.* (1999)) showed that mouse early macrophages express the M-CSF receptor gene, but not certain other markers of classical, monocyte-derived macrophages. Our present work further supports the M-CSF receptor as the most universal macrophage marker known so far, both across the various macrophage populations in the mouse and across species, from fish to mammals.

Mammalian M-CSF is best known as a key proliferation, differentiation, and survival factor for monocytes/macrophages, but it also is a chemokinetic and chemotactic factor for these cells (Webb *et al.*, 1996). M-CSF-deficient mice are deficient in several postnatal tissue macrophage populations, which were therefore classified as M-CSF-dependent (Cecchini *et al.*, 1994). However, the nature of this M-CSF dependence, among the several potential effects of M-CSF on the macrophage lineage, was not resolved.

Here in the zebrafish embryo, the direct observation of M-CSF receptor-deficient early macrophages in the yolk sac revealed no obvious behavioral deficiency in terms of proliferation and survival, nonspecific motility, and endocytic or scavenging abilities.

We do not think that M-CSF promotes the spreading of

early macrophages in embryonic tissues through a mere nonspecific stimulation of their motility (i.e., a chemokinetic effect), because *panther* early macrophages fail to colonize even target tissues that are very close to their site of residency, such as yolk sac epidermis and retina, and later the regressing hatching gland. We therefore propose that all tissues that become colonized in the wild-type attract macrophages actively, by secreting M-CSF as a chemoattractant. In the *panther* mutant, early macrophages eventually colonize the optic tectum and forebrain with a 1- to 4-day delay, and probably the retina even later, and they do so in relative numbers quite similar to the wild type. Since we found that numerous apoptotic bodies accumulate in these tissues as long as they lack microglial cells, we suggest that macrophages may be finally attracted there by signals emanating either from these apoptotic bodies, or from distress calls from neurons that have been missing the trophic support of microglia during 1–4 days. Further work will be necessary to discriminate whether these numerous apoptotic bodies correspond to cell death events also occuring in wild-type embryo, but normally eliminated as they come up by early microglia, or whether they reflect neuronal cell death caused specifically in *panther* by the transient lack of early microglial trophic support. *Panther* mutants are viable and fertile, but this does not mean that the transient absence of macrophages in the brain, retina, and other tissues is of no developmental consequence. M-CSF-deficient and ApoE-deficient mice are also viable and have apparently normal brains. It took years to realize that they actually suffer important cognitive and sensory deficits (Pollard, 1997; Fullerton *et al.*, 1998; Krzywkowski *et al.*, 1999). Such a prospect will deserve careful investigation in the *panther* mutant.

ACKNOWLEDGMENTS

P.H. is grateful to C. Petit, Head of the U.G.D.S. at Institut Pasteur, for her constant support. We thank D. Parichy for the *panther* mutant, L. Zon for the *fms* probe, and S. Easter for helpful discussions. B.T. and C.T. thank V. Heyer and T. Steffan for technical assistance. This work was supported by funds from the Institut National de la Santé et de la Recherche Médicale, the Centre National de la Recherche Scientifique, the Hôpital Universitaire de Strasbourg, the Association pour la Recherche sur le Cancer, and the Ligue Nationale Contre le Cancer.

REFERENCES

Allison, A. C., and Young, M. R. (1969). Vital staining and fluorescence microscopy of lysosomes. In "Lysosomes in Biology and Pathology" (J. T. Dingle and H. B. Fell, Eds.), pp. 600–628. North-Holland, Amsterdam.

Ashwell, K. (1989). Development of microglia in the albino rabbit retina. *J. Comp. Neurol.* **287,** 286–301.

Ashwell, K., Holländer, H., Streit, W., and Stone, J. (1989). The appearance and distribution of microglia in the developing retina of the rat. *Visual Neurosci.* **2,** 437–448.

Ashwell, K. (1991). The distribution of microglia and cell death in the fetal rat forebrain. Dev. Brain Res. **58,** 1–12.

Babin, P. J., Thisse, C., Durliat, M., André, M., Akimenko, M.-A., and Thisse, B. (1997). Both apolipoprotein E and A-I genes are present in a non-mammalian vertebrate and are highly expressed during embryonic development. *Proc. Natl. Acad. Sci. USA* **94,** 8622–8627.

Bechmann, I., and Nitsch, R. (2000). Involvment of non-neuronal cells in entorhinal-hippocampal reorganization following lesions. *Ann. N.Y. Acad. Sci.* **911,** 192–206.

Boyles, J. K., Pitas, R. E., Wilson, E., Mahley, R. M., and Taylor, J. M. (1985). Apolipoprotein E associated with astrocytic glia of the central nervous system and with nonmyelinating glia of the peripheral nervous system. *J. Clin. Invest.* **76,** 1501–1513.

Burudi, E. M., Riese, S., Stahl, P. D., and Regnier-Vigouroux, A. (1999). Identification and functional characterization of the mannose receptor in astrocytes. *Glia* **25,** 44–55.

Cecchini, M. G., Dominguez, M. G., Mocci, S., Wetterwald, A., Felix, R., Fleisch, H., Chisholm, O., Hofstetter, W., Pollard, J. W., and Stanley, E. R. (1994). Role of colony stimulating factor-1 in the establishment and regulation of tissue macrophages during postnatal development of the mouse. *Development* **120,** 1357–1372.

Cuadros, M., Garcia-Martin, M., Martin, C., and Rios, A. (1991). Haemopoietic phagocytes in the early differentiating avian retina. *J. Anat.* **177,** 145–158.

Cuadros, M. A., Coltey, P., Nieto, M. C., and Martin, C. (1992). Demonstration of a phagocytic cell system belonging to the hemopoietic lineage and originating from the yolk sac in the early avian embryo. *Development* **115,** 157–168.

Cuadros, M. A., Martin, C., Coltey, P., Almendros, A., and Navascues, J. (1993). First appearance, distribution, and origin of macrophages in the early development of the avian central nervous system. *J. Comp. Neurol.* **330,** 113–129.

Dowding, A. J., Maggs, A., and Scholes, J. (1991). Diversity amongst the microglia in growing and regenerating fish CNS: Immunohistochemical characterization using FL.1, an anti-macrophage monoclonal antibody. *Glia* **4,** 345–364.

Dowding, A. J., and Scholes, J. (1993). Lymphocytes and macrophages outnumber oligodendroglia in normal fish spinal chord. *Proc. Natl. Acad. Sci. USA* **90,** 10183–10187.

Easter, S. S. (1986). Rules of retinotectal mapmaking. *BioEssays* **5,** 157–162.

Easter, S. S., and Nicola, G. N. (1996). The development of vision in the zebrafish (*Danio rerio*). *Dev. Biol.* **180,** 646–663.

Florey, H. W. (1968). "General Pathology," Fifth Edition. Lloyd–Luke, London.

Fullerton, S. M., Strittmatter, W. J., and Matthew, W. D. (1998). Peripheral sensory nerve defects in apolipoprotein E knockout mice. *Exp. Neurol.* **153,** 156–163.

Giulian, D., and Baker, T. J. (1986). Characterization of amoeboid microglia isolated from developing mammalian brain. *J. Neurosci.* **6,** 2163–2178.

Gordon, S. (1995). The macrophage. *BioEssays* **17,** 977–986.

Gutman, C. R., Strittmatter, W. J., Weisgraber, K. H., and Matthew, W. D. (1997). Apolipoprotein E binds to and potentiates the biological activity of ciliary neurotrophic factor. *J. Neurosci.* **17,** 6114–6121.

Hashimoto, S., Suzuki, T., Dong, H. Y., Yamazaki, N., and Matsushima, K. (1999). Serial analysis of gene expression in human monocytes and macrophages. *Blood* **94,** 837–844.

Hauptmann, G., and Gerster, T. (1994). Two color whole-mount in situ hybridization on zebrafish and Drosophila embryos. *Trends Genet.* **10,** 266.

Herbomel, P., Thisse, B., and Thisse, C. (1999). Ontogeny and behavior of early macrophages in the zebrafish embryo. *Development* **126,** 3735–3745.

Isogai, S., Horiguchi, M., and Weinstein, B. M. (2001). The vascular anatomy of the developing zebrafish: An atlas of embryonic and early larval development. *Dev. Biol.* **230,** 278–301.

Jones, S. L., Wang, J., Turck, C. W., and Brown, E. J. (1998). A role for the actin-bundling protein L-plastin in the regulation of leukocyte integrin function. *Proc. Natl. Acad. Sci. USA* **95,** 9331–9336.

Kaethner, R. J., and Stuermer, C. A. (1997). Dynamics of process formation during differentiation of tectal neurons in embryonic zebrafish. *J. Neurobiol.* **32,** 627–639.

Kalman, M. (1998). Astroglial architecture of the carp (*Cyprinus carpio*) brain as revealed by immunohistochemical staining against glial fibrillary acidic protein (GFAP). *Anat. Embryol.* **198,** 409–433.

Krzywkowski, P., Ghribi, O., Gagne, J., Chabot, C., Kar, S., Rochford, J., Massicotte, G., and Poirier, J. (1999). Cholinergic systems and long-term potentiation in memory-impaired apolipoprotein E-deficient mice. *Neuroscience* **92,** 1273–1286.

Lichanska, A. M., and Hume, D. A. (2000). Origins and functions of phagocytes in the embryo. *Exp. Hematol.* **28,** 601–611.

Lichanska, A. M., Browne, C. M., Henkel, G. W., Murphy, K. M., Ostrowski, M. C., McKercher, S. R., Maki, R. A., and Hume, D. A. (1999). Differentiation of the mononuclear phagocyte system during mouse embryogenesis: The role of transcription factor PU.1. *Blood* **94,** 127–138.

Misson, J-P., Takahashi, T., and Caviness, V. S. (1991). Ontogeny of radial and other astroglial cells in murine cerebral cortex. *Glia* **4,** 138–148.

Mizoguchi, S., Takahashi, K., Takeya, M., Naito, M., and Morioka, T. (1992). Development, differentiation, and proliferation of epidermal Langerhans cells in rat ontogeny studied by a novel monoclonal antibody against epidermal Langerhans cells, RED-1. *J. Leukoc. Biol.* **52,** 52–61.

Parichy, D. M., Ransom, D. G., Paw, B., Zon, L. I., and Johnson, S. L. (2000). An orthologue of the kit-related gene fms is required for development of neural crest-derived xanthophores and a subpopulation of adult melanocytes in the zebrafish *Danio rerio*. *Development* **127,** 3031–3044.

Poirier, J. (1994). Apolipoprotein E in animal models of CNS injury and in Alzheimer's disease. *Trends Neurosci.* **17,** 525–530.

Pollard, J. W. (1997). Role of Colony-Stimulating Factor-1 in reproduction and development. *Mol. Reprod. Dev.* **46,** 54–61.

Rodriguez, M., and Driever, W. (1997). Mutations resulting in transient and localized degeneration in the developing zebrafish brain. *Biochem. Cell Biol.* **75,** 579–600.

Schmitt, E. A., and Dowling, J. E. (1999). Early retinal development in the zebrafish. *Danio rerio*: light and electron microscopic analyses. *J. Comp. Neurol.* **404,** 515–536.

Soos, J. M., Morrow, J., Ashley, T. A., Szente, B. E., Bikoff, E. K., and Zamvil, S. S. (1998). Astrocytes express elements of the class II endocytic pathway and process central nervous system autoantigen for presentation to encephalitogenic T cells. *J. Immunol.* **161,** 5959–5966.

Sorokin, S. P., Hoyt, R. F., Blunt, D. G., and McNelly, N. A. (1992a). Macrophage development: II. Early ontogeny of macrophage populations in brain, liver, and lungs of rat embryos as revealed by a lectin marker. *Anat. Rec.* **232,** 527–550.

Sorokin, S. P., McNelly, N. A., and Hoyt, R. F. (1992b). CFU-rAM, the origin of lung macrophages, and the macrophage lineage. *Am. J. Physiol.* **263,** L299–L307.

Takahashi, K., Yamamura, F., and Naito, M. (1989). Differentiation, maturation, and proliferation of macrophages in the mouse yolk sac. *J. Leukoc. Biol.* **45,** 87–96.

Takahashi, K., Naito, M., and Takeya, M. (1996). Development and heterogeneity of macrophages and their related cells through their differentiation pathways. *Pathol. Int.* **46,** 473–485.

Velasco, A., Jimeno, D., Lillo, C., Caminos, E., Lara, J. M., and Aijon, J. (1999). Enzyme histochemical identification of microglial cells in the retina of a fish (*Tinca tinca*). *Neurosci. Lett.* **263,** 101–104.

Ward, S. A., Ransom, P. L., and Thomas, W. E. (1991). Characterization of ramified microglia in tissue culture: Pinocytosis and motility. J. Neurosci. Res. **29,** 13–28.

Webb, S. E., Pollard, J. W., and Jones, G. E. (1996). Direct observation and quantification of macrophage chemoattraction to the growth factor CSF-1. *J. Cell Sci.* **109,** 793–803.

Werb, Z., and Chin, J. R. (1983). Apolipoprotein E is synthesized and secreted by resident and thioglycollate-elicited macrophages but not by pyran copolymer- or bacillus Calmette-Guerin-activated macrophages. *J. Exp. Med.* **158,** 1272–1293.

Received for publication April 13, 2001
Accepted July 5, 2001
Published online September 13, 2001